

# Journal of Biomedical Optics

BiomedicalOptics.SPIEDigitalLibrary.org

## Porcine skin damage thresholds and histological damage characteristics from 1319-nm laser radiation

Luguang Jiao  
Jiarui Wang  
Yan Fan  
Zaifu Yang

**SPIE.**

Luguang Jiao, Jiarui Wang, Yan Fan, Zaifu Yang, "Porcine skin damage thresholds and histological damage characteristics from 1319-nm laser radiation," *J. Biomed. Opt.* **24**(9), 095003 (2019), doi: 10.1117/1.JBO.24.9.095003.

# Porcine skin damage thresholds and histological damage characteristics from 1319-nm laser radiation

Luguang Jiao,\* Jiarui Wang, Yan Fan, and Zaifu Yang\*  
Beijing Institute of Radiation Medicine, Beijing, China

**Abstract.** There is an increasing use of near-infrared lasers in biomedical applications operating in the spectrum between 1300 and 1400 nm. To corroborate and expand the existing safety data for skin exposure to lasers in this wavelength region, the *in-vivo* ED<sub>50</sub> damage thresholds were determined in Guizhou miniature pigs for 1319-nm laser radiation. Exposure durations of 0.4, 1.0, and 3.0 s and  $1/e^2$  beam diameters of 0.98 and 1.96 cm were employed. Damage lesion determinations were performed at 1- and 24 h post exposure. The Bliss probit analysis was employed to establish the ED<sub>50</sub> damage thresholds. Histopathological studies of skin damage were performed at 48 h after irradiation to reveal the damage characteristics. The skin damage thresholds at 1 h post exposure, given in peak radiant exposure, were 35.5, 36.1, and 37.1 J/cm<sup>2</sup> at exposure durations of 0.4, 1.0, and 3.0 s with the spot diameter of 0.98 cm, and 28.6 J/cm<sup>2</sup> at exposure duration of 3.0 s with the spot diameter of 1.96 cm. At 24 h post exposure, the ED<sub>50</sub>s increased slightly. Histologically, the thermal damage characteristics at the near-threshold level included gathering of the nuclear chromatin and cell vacuolation in the epidermis and deposition of blood cells in the capillary vessels. However, at the apparently above-threshold level, the damage characteristics included obvious stretching of the nuclear chromatin in the epidermis, closing of the capillary lumen, structural change of collagen fibers, and coagulative necrosis of the hair follicle cells. The damage induced by this laser could go deep into the fatty tissue. The obtained results may contribute to the knowledge base for the damage mechanisms and expand the database for the refinement of laser safety standards in the wavelength range of 1300 to 1400 nm. © The Authors. Published by SPIE under a Creative Commons Attribution 4.0 Unported License. Distribution or reproduction of this work in whole or in part requires full attribution of the original publication, including its DOI. [DOI: [10.1117/1.JBO.24.9.095003](https://doi.org/10.1117/1.JBO.24.9.095003)]

Keywords: infrared laser; 1319 nm; photothermal effects; skin damage; ED<sub>50</sub> damage thresholds.

Paper 190079RR received Mar. 20, 2019; accepted for publication Sep. 6, 2019; published online Sep. 24, 2019.

## 1 Introduction

The near-infrared (NIR) laser radiation region between 1300 and 1400 nm is a unique area in the electromagnetic spectrum for laser ocular safety.<sup>1</sup> With the wavelength increase in this region, the water absorption coefficient increases sharply from about 1.35 cm<sup>-1</sup> at 1300 nm to 13.7 cm<sup>-1</sup> at 1400 nm.<sup>2</sup> Accordingly, the most vulnerable ocular tissue changes from the retina to the cornea.<sup>3</sup> Laser technology in this wavelength region continues to develop,<sup>4-6</sup> promoting increased applications in medicine and surgery. One typical medical application is in the removal of tumor tissues using the 1318-nm high-power laser.<sup>7-11</sup> Other potential applications include nonablative skin rejuvenation treatment and neural stimulation.<sup>12,13</sup>

Considering the increasing use of NIR lasers in the wavelength range of 1300 to 1400 nm,<sup>7-13</sup> it is important that they are used safely and that their use is not unnecessarily restricted. For safe use, commercial laser products must comply with specified safety standards, such as the American National Standards Institute Z136 series.<sup>14</sup> The safety standards establish the exposure limits or maximum permissible exposures (MPEs), which are primarily based on damage thresholds of eye and skin, determined through experiments in appropriate animal models.<sup>15</sup> In the past several decades, ocular bioeffects studies for the 1300- to 1400-nm NIR lasers have revealed some unique damage characteristics that are obviously different from those of

the visible or the far-infrared (IR) lasers. First, the absorption of incident laser energy in this region is more evenly distributed across the ocular media.<sup>16</sup> Damage may be induced in one or more of the cornea, lens, and retina/choroid, depending on the precise exposure parameters.<sup>1,3</sup> Second, strong spot dependencies exist for this wavelength region. At relatively large beam spot sizes at the cornea, threshold-level damage occurs at the back of the eye, involving the retina and the nerve fiber layers, whereas for relatively small corneal spot sizes, threshold-level damage occurs at the cornea.<sup>17</sup> Third, a retinal or corneal lesion involves the full thickness of that layer, even at the threshold level.<sup>18-21</sup> Fourth, the corneal or retinal damage thresholds can be correlated by power law functions, having similar trends with other visible or far-IR lasers.<sup>20,21</sup> Fifth, the ocular axial length is a great influential factor on the retinal damage threshold, whereas retinal pigmentation is a relatively minor factor. However, for lasers emitting visible radiation, the retinal damage threshold is significantly relevant to the retinal pigmentation, and the ocular axial length is a secondary influential factor.<sup>22</sup> Sixth, for visible radiation, the observer is aware of the light, and the blinking reflex prevents eyes from continuing to be exposed. Thus, damage thresholds should be determined for shorter exposure durations. But for NIR lasers, eyes cannot perceive the radiation, so damage thresholds should also be determined for longer exposure durations. Finally, retinal damage thresholds are determined in rabbit models at exposure durations up to 10 s, but in nonhuman primate models, no damage thresholds are determined for exposure durations longer than 0.08 s. Significant presence of a thermal lensing effect is believed to

\*Address all correspondence to Luguang Jiao, E-mail: [jiaoluguang001@163.com](mailto:jiaoluguang001@163.com); Zaifu Yang, E-mail: [yangzf@bmi.ac.cn](mailto:yangzf@bmi.ac.cn)

explain this variance.<sup>23–26</sup> These characteristics are remarkably different from the ocular damage induced by other wavelength ranges and receive increasing concerns.

Existing reports give considerable attention to ocular damages because of the great importance of vision. However, the skin is the largest organ of the body and the most probable to be accidentally irradiated by laser. The human skin consists of three layers, including epidermis, dermis, and subcutaneous.<sup>27</sup> The epidermis is in the outermost layer of living cells. New skin cells are formed regularly so that the epidermis renews itself about every 4 weeks and the surface layer of epidermis is made up of dead skin cells. This surface layer is called the stratum corneum and has a thickness of about 10 to 20  $\mu\text{m}$ . Keratin is formed in the epidermis. The dermis contains collagen and elastin, as well as blood vessels and nerve cells. The subcutaneous layer is located in the innermost layer of the skin and is mostly fatty tissue. The thickness of the subcutaneous layer varies strongly in body regions. Laser propagation in skin is different from eyes, mainly because of the significant scattering effect.<sup>28</sup> Many efforts have been made to measure the skin optical properties, including the refractive index, the scattering coefficient, the absorption coefficient, and the anisotropy.<sup>29–31</sup> These data can be employed in a complex Monte Carlo model to analyze the light distribution variations with laser wavelengths.<sup>28</sup> However, for the setting/refinement of laser safety standards, experimentally determining damage thresholds in an appropriate animal model is the primary task. Over the past decades, several *in vivo* studies,<sup>32–37</sup> using the porcine skin model, have been conducted for the purpose of determining the dose associated with 50% probability of the minimum visible lesion ( $ED_{50}$ ), which is commonly considered as a damage threshold. In previous skin studies, the experimental and simulation results from Chen et al.<sup>32–34</sup> were presented for a 2000-nm thulium fiber laser for various exposure durations (0.25 to 2.5 s) and incident beam diameters (5 to 15 mm). Oliver et al.<sup>35</sup> determined the skin damage thresholds from a 1940-nm thulium fiber laser, employing exposure durations from 10 ms to 10 s and beam diameters of 4.8 to 18 mm. Cain et al.<sup>36</sup> reported damage threshold measurements from two pulsed 1540-nm Er: glass lasers (600  $\mu\text{s}$  and 31 ns) for three different spot sizes (0.7, 1.0, and 5.0 mm). Vincelette et al.<sup>37</sup> reported results from experiments to determine the damage thresholds for the wavelength of 1070 nm for a range of beam diameters (0.6 to 9.5 cm) and exposure durations (10 ms to 10 s). For the 1300- to 1400-nm NIR lasers, only two special reports about skin damage are found at present.<sup>38,39</sup> Cain et al.<sup>38</sup> determined the damage thresholds for two pulsed 1315-nm lasers at different beam spot sizes (350  $\mu\text{s}$  with beam diameters of 0.7 and 1.3 mm, 50 ns with beam diameter of 5.0 mm). And the experimental and simulation results from Oliver et al.<sup>39</sup> were presented for a 1319-nm continuous-wave Nd:YAG laser for exposure durations of 0.25, 1.0, 2.5, and 10 s and beam diameters of  $\sim$ 0.6 and 1 cm. Despite these skin damage studies in the 1300- to 1400-nm NIR range, two problems are believed to remain unexplored. First, the two existing reports focus on two distinct exposure duration regions and no overlapping exists between them;<sup>38,39</sup> thus, the accuracy of these damage data cannot be evaluated. Other studies are essential to validate the existing data and expand the damage threshold database, considering the widespread use of high-power laser systems in this region and the risk of skin damages.<sup>7–13</sup> Second, no skin histopathological studies have been conducted for the 1300- to 1400-nm NIR lasers, leading to the fact that the laser-induced

tissue damage characteristics and the damage extent at different exposure levels have remained unknown.

Considering the above two deficiencies, we conducted a series of experiments using a continuous-wave laser with the wavelength of 1319 nm, to determine the skin damage thresholds and reveal the damage characteristics and extent by performing histopathological observations. The results presented in this paper may contribute to the knowledge base for the damage mechanisms and the refinement of laser safety standard in the NIR range.

## 2 Materials and Methods

### 2.1 Experimental Setup

Figure 1 shows the schematic drawing of the laser exposure setup. The laser employed for this study was a diode-pumped continuous-wave Nd:YAG laser at the wavelength of 1319 nm (Fujian Institute of Research on the Structure of Matter, Chinese Academy of Science, Fujian, China). The maximum output of the CW 1319-nm laser was about 80 W, with power stability within  $\pm 2\%$  for 1-h operating time. An electronically controlled mechanical shutter was employed to control the exposure duration. A constant proportion of the laser power was reflected onto the 1# laser power meter (3A, Ophir, Jerusalem, Israel) using a beam splitter placed slightly off the axis. The splitter was a glass plate made of fused quartz. The main purpose of using the splitter was to monitor the stability of the laser power during the experimental process. Before the animal was positioned, the 2# calibrated laser power meter (30A, Ophir, Jerusalem, Israel) was placed at the target surface to directly receive the power, which would be perpendicularly incident on the porcine skin. By changing the driving current of the laser system, the desired laser power could be reached. Meanwhile, the power at the reference was obtained through the 1# power meter. In the subsequent exposure experiments, we could monitor the laser stability by observing the power readings displayed by the 1# laser power meter. Two low-power 655-nm laser pointers, crossed at the center of the selected laser spot, facilitated the targeting of the invisible 1319-nm laser. A focusing lens, with a focal length of 300 mm, was positioned to change the laser spot size. The irradiance of the laser spot was nearly Gaussian-distributed, which was characterized through the knife-edge method.<sup>16</sup> The  $1/e^2$  beam diameter arriving at the focusing lens was about 1.20 cm, and the selected  $1/e^2$  beam diameters were measured to be  $0.98 \pm 0.01$  and  $1.96 \pm 0.02$  cm at two target planes by repeated measurements prior to exposure. The distances between the lens and the target planes with the two spot sizes (0.98/1.96 cm) were about 108.2 and 161.3 cm, respectively. The  $1/e^2$  diameter refers to the diameter of the smallest circle, which contains 86.5% of the total laser power. We selected the two beam diameters mainly for the following reasons. According to previous reports,<sup>32–35</sup> skin damage thresholds are dependent on laser spot size. The use of large beam diameters results in a measured threshold under conditions near one-dimensional limit of heat transfer in the skin. Thresholds under these conditions should therefore approach the lower possible radiant requirement for thermal damage. In this way, the MPEs in safety standards could be appropriately formulated based on the determined damage values.<sup>27</sup> Previous reports also indicate that beam diameter of about 1 cm is large enough to obtain lower damage values. So we selected the beam diameter of about 1 cm. However, we also wanted to investigate whether

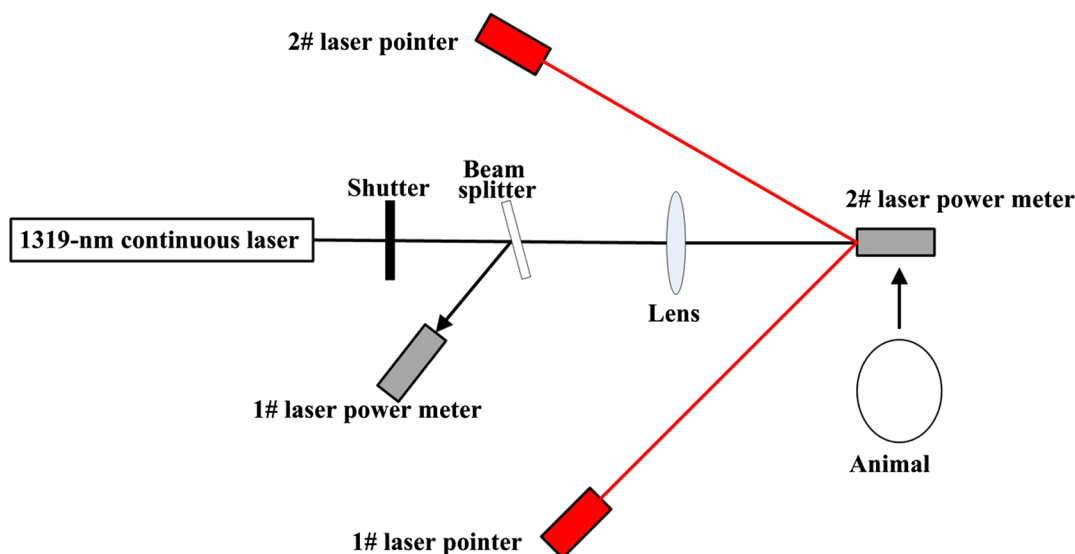


**Fig. 1** Schematic drawing of the laser exposure setup for the determination of porcine skin damage thresholds at the wavelength of 1319 nm. The  $1/e^2$  beam diameter arriving at the focusing lens was about 1.20 cm, and the selected  $1/e^2$  beam diameters were measured to be  $0.98 \pm 0.01$  and  $1.96 \pm 0.02$  cm at two target planes by repeated measurements prior to exposure. The distances between the lens and the target planes with the two spot sizes (0.98 and 1.96 cm) were about 108.2 and 161.3 cm, respectively.

the damage thresholds would obviously decrease when the beam diameter continue to increase, and therefore another beam diameter of about 2 cm was selected for comparison.

## 2.2 Animal Subjects

Guizhou miniature pigs of either sex, having white hair and skin, were selected for skin damage determinations. The animal study was approved by the ethics review board of the Academy of Military Medical Science, Beijing, China. All animals, weighing 15 to 20 kg, were procured and maintained in the Center for Laboratory Animal Medicine and Care, Beijing, China, and used in accordance with the institutional guidelines of the Animal Care and Use Committee. To ensure that the subjects did not experience pain and distress, all pigs were anesthetized with an intramuscular injection of Sumianxin II (0.15 ml/kg). After the animal reached a surgical plane of anesthesia, electric clippers were used to remove hair from the flank. The flank was cleaned with soap and warm water, rinsed, and dried with a lint-free disposable cloth. A grid pattern was drawn on the flank of the pigs using a black permanent marker with grid spacing of about 3.0 to 4.0 cm for the nominal laser beam diameters of 0.98 and 1.96 cm. The flank area was selected mainly for following facts. Eggleston et al.<sup>40</sup> measured the epidermis thickness of different skin areas of Yucatan miniature pig and human. It is shown that the mean thickness of flank epidermis is  $68 \pm 34 \mu\text{m}$ , which is comparable to the thickness of human epidermis of the face ( $68 \pm 26 \mu\text{m}$ ), neck ( $68 \pm 24 \mu\text{m}$ ), and arms ( $68 \pm 21 \mu\text{m}$ ). Therefore, it is concluded that the flank regions are better suited to laser injury studies. For this reason, almost all existing reports select the flank area of miniature pig to determine the skin damage thresholds induced by laser.<sup>32-39</sup>

## 2.3 Experimental Procedures and Data Analysis

For laser exposures, the anesthetized animals were placed in a customized holder where they were positioned with the aid of

the low-power laser pointers. The holder was mounted on rails and motorized for rapid and repeatable horizontal position adjustment of the test animals. The vertical position could be adjusted by a hand-controlled elevation system. In this way, each grid that had been drawn on the flanks of the pigs was sequentially irradiated. The exposure durations selected for the spot size of 0.98 cm were 0.4, 1.0, and 3.0 s. For the spot size of 1.96 cm, the 3.0-s exposure duration was selected. Once the positions corresponding to the selected beam diameters (0.98 and 1.96 cm) were determined, the two low-power 655-nm laser pointers were placed to make the two beams crossing at the center of the 1319-nm laser spot. When exposing the pigs to laser radiation, we adjusted the animal position so that the beam cross-point of the two 655-nm laser pointers was at the skin surface. The location error of the skin surface was no more than  $\pm 3$  mm along the incident 1319-nm laser direction. We could estimate the maximum variance for the spot size along the 6-mm range. Because the distance between the two target planes for the two spot sizes (0.98 and 1.96 cm) was 53.1 cm, the maximum variance along a 6-mm range would be about 0.01 cm ( $0.98/53.1 \times 0.6$  cm). Therefore, it could be concluded that the beam diameter on the skin surface would have a negligible variance due to location errors.

For each combination of spot size and exposure duration, a pilot study was first conducted to generate damages in different exposure levels, from no skin damage to obvious skin burns. From the postexposure reading, the approximate range of the damage threshold for each condition was estimated. Based on the estimation, four to five different power levels were chosen in the subsequent experiment to determine the damage threshold. For example, for the beam diameter of 0.98 cm and the exposure duration of 0.4 s, eight power levels, including 80, 70, 60, 50, 40, 30, 20, and 10 W, were first employed to irradiate the pig skin. Results showed that the irradiated skin tissue were severely damaged for power levels of 80, 70, and 60 W and no damage could be found for power levels of 10, 20, and 30 W.

For power level of 50 W, the skin was also damaged but was not very severe. Therefore, the ED<sub>50</sub> damage threshold should be located in the range of 30 to 50 W, and we selected five power levels from 30 to 50 W to determine the damage threshold. A total of 16 pigs were employed. For each combination of laser spot diameter and exposure duration, four pigs were involved. At every selected power level, a total of 40 exposures were irradiated on the four porcine skin surfaces, with 10 exposures for each pig in the group. The laser parameters and corresponding experimental conditions are shown in the Table 1.

Following each exposure session, lesion/no lesion determinations were made for each exposure site by three experienced investigators, with at least two of three in agreement to confirm a positive reading. Any change in the appearance of the skin surface was recorded as a lesion, including erythema, blistering, or change in pigmentation viewed by the eye. Examinations were performed at 1 and 24 h post exposure. The lesion/no lesion data were collected and analyzed using the SAS statistical package (version 6.12, SAS Institute, Inc., Cary, North Carolina). Specifically, using the collected damage probabilities at different laser power levels, the dose–response curve could be obtained, and then the widely accepted Bliss probit analysis was performed to determine the ED<sub>50</sub> thresholds, fiducial limits at

the 95% confidence level, and probit slopes  $S$  (ED<sub>84</sub>/ED<sub>50</sub>).<sup>15</sup> The ED<sub>50</sub> refers to the effective dose corresponding to 50% damage probability. Three methods could be employed to express the ED<sub>50</sub> thresholds and fiducial limits at the 95% confidence, including the incident laser power, the total energy on the animal skin and the central peak radiant exposure for the Gaussian spot, as shown by Tables 2 and 3. The peak radiant exposure is determined according to the following equation:  $8ED_{50}t/(\pi D^2)$ . In the equation, ED<sub>50</sub>,  $t$ , and  $D$  are the damage thresholds expressed in power, exposure duration, and  $1/e^2$  spot diameter, respectively. One point to note is that there are two methods for specifying the slope of the probit plot. The first definition is the conventional mathematical meaning of slope, i.e., the change in probability of an effect divided by the change in dose, and termed the “real slope” (RS). The other method commonly used in the laser bioeffects literature is to define the probit slope  $S$  as the ratio of the ED<sub>84</sub> value divided by the ED<sub>50</sub> value. The two definitions are related by  $RS = 1/\log S$ .<sup>15</sup>

A digital camera (EOS 760D, Canon, Japan) was used to capture the skin images. Furthermore, histopathological studies were also performed. One pig was euthanized at 48 h after exposure. Other pigs were preserved and returned back to the animal center for other experiments. After the euthanasia, the skin

**Table 1** Laser parameters and experimental conditions.

| Laser spot diameters and exposure durations selected |                        |                           |                                 |  |              |                         |                        |
|--|------------------------|---------------------------|---------------------------------|--|--------------|-------------------------|------------------------|
| 1/e <sup>2</sup> diameter (cm)                       | Exposure durations (s) | Power levels selected (W) | Corresponding energy levels (J) | Peak radiant exposure (J/cm <sup>2</sup> ) | Group number | Involved animal numbers | Total exposure numbers |
| 0.98   | 0.4                    | 30.0                      | 12.0                            | 31.8                                       | 1#           | 4                       | 200                    |
|  |                        | 35.0                      | 14.0                            | 37.1                                       |              |                         |                        |
|  |                        | 40.0                      | 16.0                            | 42.4                                       |              |                         |                        |
|  |                        | 45.0                      | 18.0                            | 47.7                                       |              |                         |                        |
|  |                        | 50.0                      | 20.0                            | 53.0                                       |              |                         |                        |
| 0.98   | 1.0                    | 12.0                      | 12.0                            | 31.8                                       | 2#           | 4                       | 160                    |
|  |                        | 15.0                      | 15.0                            | 39.8                                       |              |                         |                        |
|  |                        | 18.0                      | 18.0                            | 47.7                                       |              |                         |                        |
|  |                        | 21.0                      | 21.0                            | 55.7                                       |              |                         |                        |
| 0.98   | 3.0                    | 3.0                       | 9.0                             | 23.9                                       | 3#           | 4                       | 200                    |
|  |                        | 4.0                       | 12.0                            | 31.8                                       |              |                         |                        |
|  |                        | 5.0                       | 15.0                            | 39.8                                       |              |                         |                        |
|  |                        | 6.0                       | 18.0                            | 47.7                                       |              |                         |                        |
|  |                        | 7.0                       | 21.0                            | 55.7                                       |              |                         |                        |
| 1.96   | 3.0                    | 12.0                      | 36.0                            | 23.9                                       | 4#           | 4                       | 160                    |
|  |                        | 16.0                      | 48.0                            | 31.8                                       |              |                         |                        |
|  |                        | 20.0                      | 60.0                            | 39.8                                       |              |                         |                        |
|  |                        | 24.0                      | 72.0                            | 47.7                                       |              |                         |                        |

**Table 2** Skin damage thresholds induced by 1319-nm laser for lesions 1 h after exposure.

| $1/e^2$ diameter (cm) | Exposure durations (s) | Number of exposures (Yes, No) | ED50 damage threshold (fiducial limits at the 95% confidence) in power (W) | ED <sub>50</sub> damage threshold (fiducial limits at the 95% confidence) in energy (J) | Probit slope (ED <sub>84</sub> /ED <sub>50</sub> ) | ED <sub>50</sub> damage threshold (fiducial limits at the 95% confidence) in peak radiant exposure (J/cm <sup>2</sup> ) |
|-----------------------|------------------------|-------------------------------|--|---|--|---|
| 0.98                  | 0.4                    | 200 (150, 50)                 | 33.5 (32.5, 34.5)  | 13.4 (13.0, 13.8)   | 1.10   | 35.5 (34.5, 36.6)   |
| 0.98                  | 1.0                    | 160 (115, 45)                 | 13.6 (12.9, 14.2)  | 13.6 (12.9, 14.2)   | 1.19   | 36.1 (34.2, 37.7)   |
| 0.98                  | 3.0                    | 200 (108, 92)                 | 4.68 (4.45, 4.92)  | 14.0 (13.4, 14.8)   | 1.23   | 37.1 (35.5, 39.2)   |
| 1.96                  | 3.0                    | 160 (114, 46)                 | 14.4 (13.6, 15.1)  | 43.2 (40.8, 45.3)   | 1.19   | 28.6 (27.0, 30.0)   |

**Table 3** Skin damage thresholds induced by 1319-nm laser for lesions 24 h after exposure.

| $1/e^2$ diameter (cm) | Exposure durations (s) | Number of exposures (Yes, No) | ED50 damage threshold (fiducial limits at the 95% confidence) in power (W) | ED <sub>50</sub> damage threshold (fiducial limits at the 95% confidence) in energy (J) | Probit slope (ED <sub>84</sub> /ED <sub>50</sub> ) | ED <sub>50</sub> damage threshold (fiducial limits at the 95% confidence) in peak radiant exposure (J/cm <sup>2</sup> ) |
|-----------------------|------------------------|-------------------------------|--|---|--|---|
| 0.98                  | 0.4                    | 200 (126, 74)                 | 36.7 (35.7, 37.5)  | 14.7 (14.3, 15.0)   | 1.08   | 38.9 (37.9, 39.8)   |
| 0.98                  | 1.0                    | 160 (93, 67)                  | 15.4 (14.9, 15.9)  | 15.4 (14.9, 15.9)   | 1.10   | 40.8 (39.5, 42.2)   |
| 0.98                  | 3.0                    | 200 (80, 120)                 | 5.46 (5.26, 5.66)  | 16.4 (15.8, 17.0)   | 1.14   | 43.4 (41.9, 45.1)   |
| 1.96                  | 3.0                    | 160 (98, 62)                  | 16.0 (15.2, 16.7)  | 48.0 (45.6, 50.1)   | 1.18   | 31.8 (30.2, 33.2)   |

tissues of the damage positions were taken and fixed in 10% neutral buffered formalin, embedded with paraffin, serially sectioned, and the sections stained with hematoxylin and eosin. Serial consecutive histological sections were cut through selected sample blocks and examined to locate the center of the damage lesion at the microscopic level. A microscope (Model BX43F, Olympus, Tokyo, Japan) was used to analyze the skin sections.

### 3 Results and Discussions

#### 3.1 Skin Damage Thresholds at Different Conditions

All the experimental conditions and the corresponding damage thresholds for the 1- and 24-h observational time points are summarized in Tables 2 and 3, respectively. The third columns in the tables list the total number of laser exposures for each combination of laser spot diameter and exposure duration. The “Yes” means that damage lesion could be found for the exposure site. And the “No” means that no damage could be found for the exposure site.

Figure 2 was a typical graph showing the probit analysis of skin damages for miniature pig. The incident beam diameter and exposure duration was 1.96 cm and 3.0 s, respectively. The red square points were experimentally determined damage probabilities at 1 h post exposure for corresponding power levels. By probit analysis, the ED<sub>50</sub>, the fiducial limits at the 95% confidence level, and the probit slope (ED<sub>84</sub>/ED<sub>50</sub>) could be determined.

Figure 3 shows the comparisons of the skin damage thresholds for lesions 1 h post exposure between this work and the Ref. 39, which presented the damage thresholds for exposure

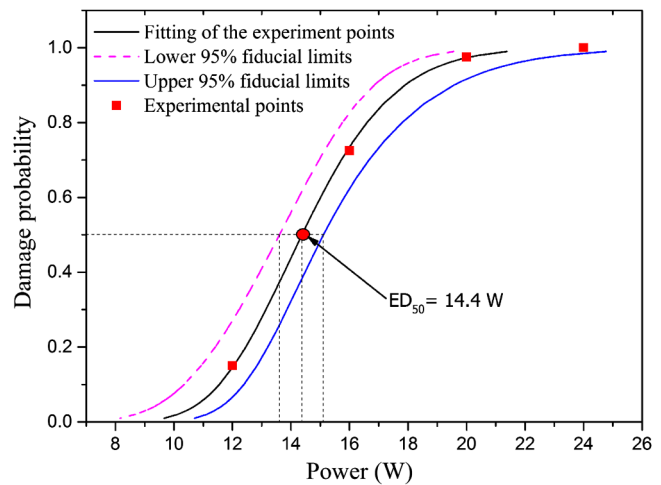


**Fig. 2** Typical graph showing the probit analysis of skin damages for Guizhou miniature pig. The incident beam diameter and exposure duration was 1.96 cm and 3.0 s, respectively. The red square points were experimentally determined damage probabilities at 1 h post exposure for corresponding power levels. By probit analysis, the ED<sub>50</sub>, the fiducial limits at the 95% confidence level, and the probit slope could be determined.

durations of 0.25, 1.0, 2.5, and 10.0 s with the  $1/e^2$  spot diameters of 0.61 and 0.97 cm, respectively. This work determined the damage thresholds for exposure durations of 0.4, 1.0, and 3.0 s with the  $1/e^2$  spot diameter of 0.98 cm, and for exposure duration of 3.0 s with the  $1/e^2$  spot diameter of 1.96 cm, respectively.

By analyzing the results presented in Tables 2 and 3 and Fig. 3, some conclusions could be drawn. First, the damage

thresholds for 24 hours post exposure are slightly higher than the results for 1 h post exposure. This is because some lesions that can be discerned at 1 h post exposure disappear at 24 h after exposure. A definitive interpretation on a cellular level for this phenomenon has not been formulated. A possible recovering process is as follows. At 1 h post exposure, some very slight damages appeared as purple spots, which may be induced by the dilation or obstruction of capillaries. At 24 h post exposure, the functions of capillaries were recovered so that the purple spots disappeared or were hard to discern. Second, the damage thresholds, expressed as peak radiant exposure, decrease as the incident spot expands in diameter. This phenomenon is determined by the heat accumulation and thermal diffusion in skin by laser irradiation. As the incident spot size is small, the temperature rise of the center area is strongly influenced by the heat diffusion to the surrounding region. With the increase of the spot size, the influence by the heat diffusion decreases and the absorbed energy is more easily to accumulate in the exposed center area, so the damage threshold decreases. Under large spot size conditions near the theoretical one-dimensional limit of heat transfer in the skin, where radial heat losses from the center of the beam-tissue interface are negligible with respect to losses due to axial heat transfer, the damage thresholds would approach the lowest possible radiant exposure ( $J/cm^2$ ) requirement for thermal damage. Third, for constant spot diameters of 0.67 and 0.97 cm, the damage thresholds expressed as total energy or peak radiant exposure keep nearly constant for exposure durations from 0.25 to about 3 s but have an obvious increase as the exposure duration increases to 10.0 s. This is also mainly determined by the effect of the heat accumulation and thermal diffusion in skin. For long exposure durations such as 10.0 s, heat diffusion from the center region to the surrounding region has a significant influence to the temperature rise in the skin by laser irradiation, and thus more energy would be accumulated to induce the skin damage, compared with the short exposure durations. This phenomenon has been explained quantitatively by Chen et al.<sup>33</sup> and Oliver et al.<sup>35,39</sup> through a complex

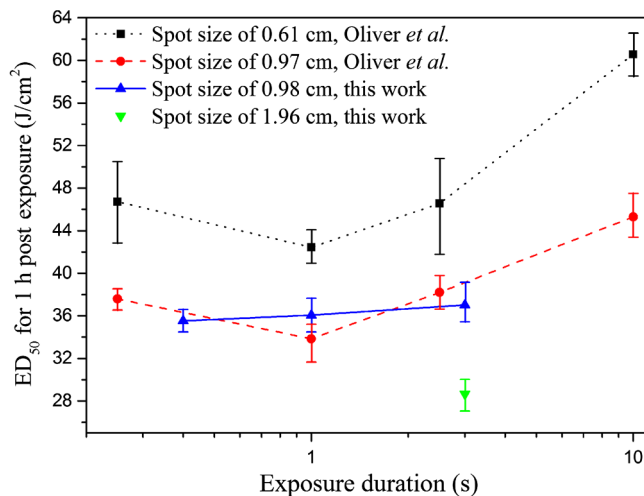


**Fig. 3** Comparisons of the skin damage thresholds for lesions 1 h after exposure, between this work and the work of Oliver et al.<sup>39</sup> Oliver et al. presented the damage thresholds for exposure durations of 0.25, 1.0, 2.5, and 10.0 s with the  $1/e^2$  spot diameters of 0.61 and 0.97 cm, respectively. This work determined the damage thresholds for exposure durations of 0.4, 1.0, and 3.0 s with the  $1/e^2$  spot diameter of 0.98 cm, and for exposure duration of 3.0 s with the  $1/e^2$  spot diameter of 1.96 cm, respectively.

numerical model that includes light transmission submodel, heat transfer submodel, and Arrhenius integral submodel. Fourth, the probit slope has generally been considered a good indication of the overall uncertainty and quality of the experimental data.<sup>15</sup> For skin damage threshold, the probit slopes are about 1.1 to 1.2 due to relatively low variations among individuals. In this investigation, the probit slopes were between 1.08 and 1.23, similar to previous report ranging from 1.01 to 1.14.<sup>39</sup> Finally, the damage thresholds determined in this paper agree well with the results from Oliver et al.,<sup>39</sup> which validate the accuracy of the published data. The data in Fig. 3 provide the solid foundation for the refinement of the safety standard.

### 3.2 Damage Characteristics Shown by Skin Pictures and Histological Sections

Figures 4(a) to 4(d) show the skin lesions at immediately, 1 h, 24 h, and 7 days post exposure. The beam diameter, the exposure duration, and the laser power was 1.96 cm, 3.0 s, and 16.0 W respectively. The radiant exposure corresponding to this

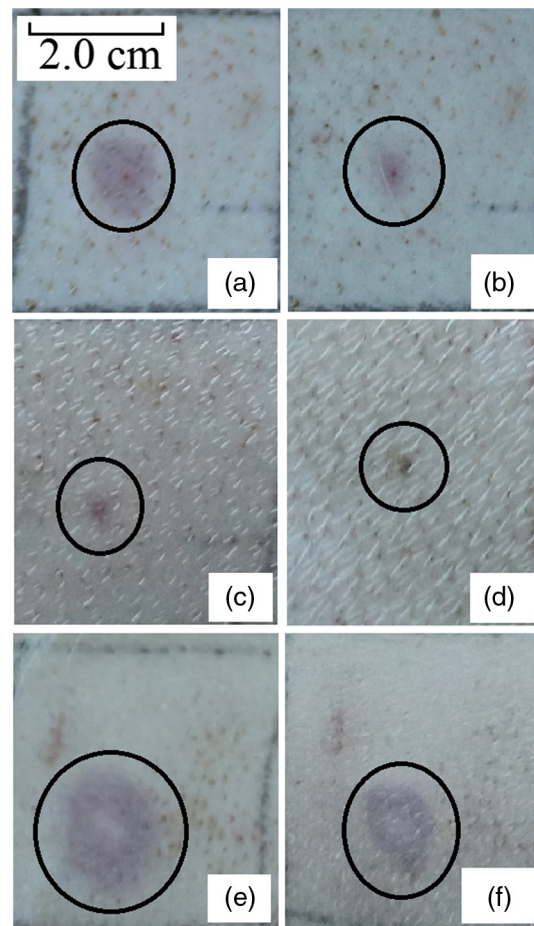


**Fig. 4** Skin damage images induced by 1319 nm continuous-wave laser. The black circles indicated the lesions. (a) Immediately post exposure, (b) 1 h post exposure, (c) 24 h post exposure, (d) 7 days post exposure, (e) immediately post exposure, and (f) 24 h post exposure. Laser conditions from (a) to (d): beam diameter was 1.96 cm, exposure duration was 3.0 s, laser power was 16.0 W, and the radiant exposure was about 1.11 times of the  $ED_{50}$  damage threshold. Laser conditions of (e) and (f): beam diameter was 1.96 cm, exposure duration was 3.0 s, laser power was 24.0 W, and the radiant exposure was about 1.67 times of the  $ED_{50}$  damage threshold.

condition was about 1.1 times of the ED<sub>50</sub> damage threshold shown in Table 2. Figures 4(e) and 4(f) show the lesions with the power of 24.0 W, about 1.67 times of the damage threshold. Lesions near the damage threshold appeared as red, flat spots at the site of irradiation immediately post exposure. Nearly all of the lesions appeared instantly after laser irradiation. Some of them disappeared at the 1 h post exposure and the area of the persisted purple lesions obviously reduced, compared to the instant appearance. At 24 h post exposure, some lesions could not be discerned, thus the damage threshold was slightly higher than that at 1 h post exposure. Dark scab was observed at 7 days post exposure, as shown in Fig. 4(d). When incident power was 1.67 times of the threshold, coagulation of the skin occurred and the damage area for this case had a much bigger size than that at the threshold level. The lesion sizes from 4(a) to 4(f) were about 1.12, 0.48, 0.29, 0.24, 1.70, and 1.32 cm.

Figure 5 shows the light micrographs of normal undamaged skin histological section and the damaged tissue sections at 48 h post exposure for different conditions. In the normal skin, as shown in Fig. 5(A), the cell nuclei of the epidermis, including the basal layer, the stratum spinosum, and stratum granulosum, stained evenly, with round or elliptical shape. The cells of the

basal layer were arranged orderly and tightly. The nuclei of dermal fibroblast, mostly with elliptical or long-elliptical shape, were stained evenly. Most of the collagen fibers arranged in nearly parallel to the skin surface and the structures were clear. Rich capillary network could be found in the junction area between the dermal papilla and the reticular dermis. Blood cells were not found in the vessels. Figure 5(B) shows the skin section corresponding to the near-threshold damage (1.11 times of the ED<sub>50</sub> damage threshold). The nuclear chromatin in the epidermis gathered with obvious cell vacuolation. Part of the basal layer detached with the dermal layer. The cell nuclei in the upper dermis layer shrank with hyperchromatism. Blood cells were deposited abundantly in the capillary vessels, and the structures of the collagen fibers were still clear. Figure 5(C) shows the skin section corresponding to the obviously above-threshold damage (1.67 times of the ED<sub>50</sub> damage threshold). Obvious stretching of the nuclear chromatin could be found, and the pyknosis, degradation, or vacuolization was not found in the epidermis. Compared to the near-threshold level, the basal layer still linked tightly with the dermal layer. In the dermal papilla and the reticular layer, the cell nuclei shrank with hyperchromatism. Closing of the capillary lumen could be noticed and no blood

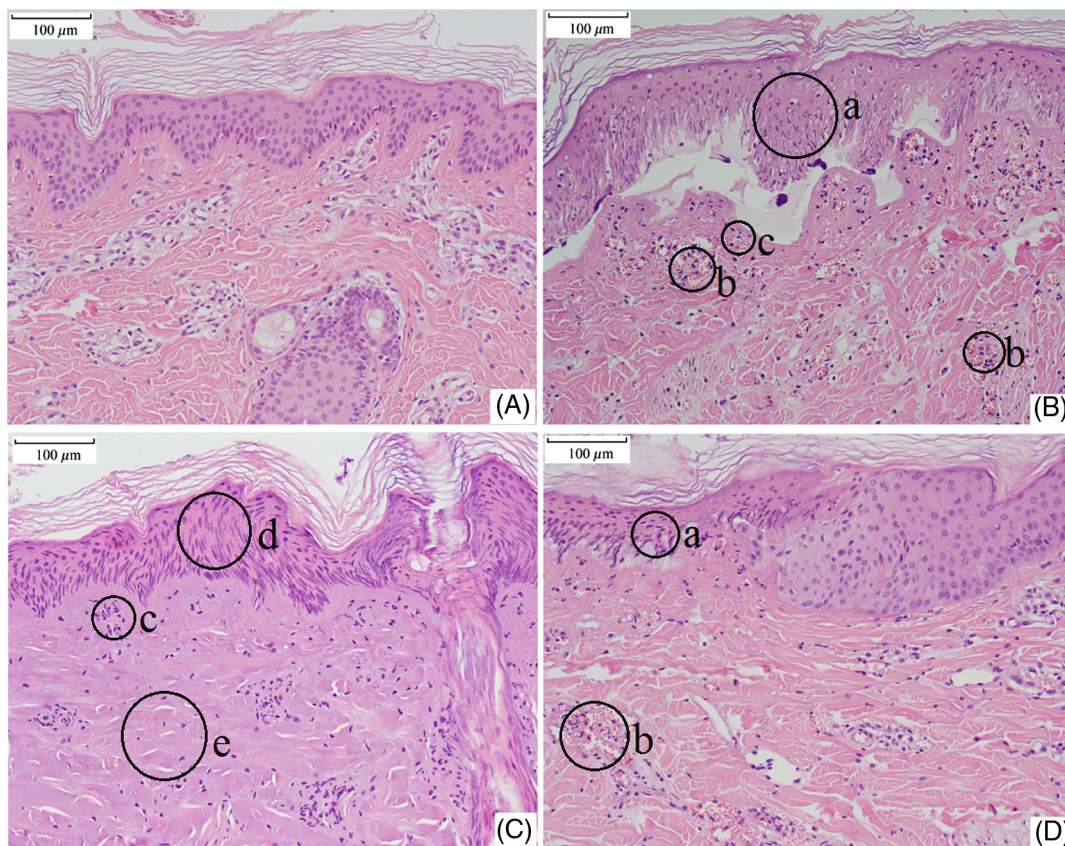


**Fig. 5** Histological sections of skin tissue. (A) Normal skin tissue. (B) Damaged skin tissue at 48 h post exposure. Laser conditions: beam diameter 1.96 cm, exposure duration 3.0 s, and laser power 16.0 W. The radiant exposure was about 1.11 times of the ED<sub>50</sub> damage threshold. (C) Skin tissue at the central region of a damage lesion at 48 h post exposure. Laser conditions: beam diameter 1.96 cm, exposure duration 3.0 s, and laser power 24.0 W. The radiant exposure was about 1.67 times of the ED<sub>50</sub> damage threshold. (D) Skin tissue at the edge region of the same lesion as (C). Laser condition was the same as (C). The specimens seen in (C) and (D) were from the same tissue section but different locations. The circles from (a) to (e) represented following damage characteristics: (a) gathered nuclear chromatin in the epidermis, (b) blood cells deposited abundantly in the capillary vessels, (c) the cell nuclei in the upper dermis layer shrank with hyperchromatism, (d) obvious stretching of the nuclear chromatin in the epidermis, and (e) the structure of the collagen fibers changed obviously with homogenization characteristic.

cells were found. The structure of the collagen fibers changed obviously, with homogenization characteristic. Coagulative necrosis was found in the hair follicle cells. However, in the edge region of the damaged lesion [Fig. 5(D)], obvious cell vacuolation could still be found in the epidermis and blood cells deposited abundantly in the capillary vessels, which was similar with the characteristics shown in Fig. 5(B). Another interesting damage characteristic was the relatively high penetration depth compared to other IR lasers with longer wavelengths such as thulium laser (around 2000 nm). As shown in Fig. 6, blood cells are deposited abundantly in the fatty layer for the damaged tissue. However, this phenomenon was not observed in the normal undamaged skin fatty tissues and was not found in other IR lasers with longer wavelengths.<sup>34</sup> In a previous report,<sup>41</sup> we have calculated the light distribution in the skin using a Monte Carlo model. It was shown that the fluence rate decreased to nearly zero at a depth of about 3 mm, which was comparable to values for visible radiation.<sup>27</sup> Thus, the damage characteristics for the 1319-nm laser were similar with visible lasers. Since ED<sub>50</sub> damage thresholds are dependent on spot sizes, we selected the damage values for different wavelengths at a nearly constant beam size (about 1.0 cm) to illustrate the influence of laser wavelength, as shown in Fig. 7. The difference for the damage

thresholds is due to different penetration depths for the three wavelengths.<sup>27</sup> Radiation will penetrate deepest into skin at the wavelength of 1070 nm among the three wavelengths; that is, most energy is needed for 1070 nm to increase the skin temperature to the critical level that generates thermal damage.

## 4 Conclusion

The porcine skin damage ED<sub>50</sub> thresholds for the 1319-nm laser were determined. For 1/e<sup>2</sup> beam spot diameter of 0.98 cm and three exposure durations of 0.4, 1.0, and 3.0 s, the ED<sub>50</sub>s at 1 h post exposure were 35.5, 36.1, and 37.1 J/cm<sup>2</sup>, respectively. For 1/e<sup>2</sup> beam spot diameter of 1.96 cm and exposure duration of 3.0 s, the ED<sub>50</sub> value at 1 h post exposure was 28.6 J/cm<sup>2</sup>. At 24 h post exposure, the ED<sub>50</sub>s increased slightly. Histological studies revealed the damage characteristics of near-threshold and apparently above-threshold lesions. The obtained results, in combination with the published damage data, can be used for the refinement of the safety standards for NIR lasers. In addition, these data may have high reference value for laser parameter selections of certain medical applications such as clinical diagnosis of pain, in which the nociceptors are simulated by laser and safe exposure doses should be demarcated to avoid skin damages.

## Disclosures

The authors have no relevant financial interests in the article and no other potential conflicts of interest to disclose.

## Acknowledgments

This study was supported by the National Natural Science Foundation of China (NSFC) (Nos. 61575221 and 61275194).

## References

1. J. A. Zuclich et al., "Ocular effects of penetrating IR laser wavelengths," *Proc. SPIE* **2391**, 112–125 (1995).
2. D. J. Segelstein, "The complex refractive index of water," Master's Thesis, University of Missouri, Kansas City (1981).
3. J. A. Zuclich, D. J. Lund, and B. E. Stuck, "Wavelength dependence of ocular damage thresholds in the near-IR to far-IR transition region: proposed revisions to MPEs," *Health Phys.* **92**(1), 15–23 (2007).
4. A. Saha et al., "Simultaneous oscillations of twelve wavelengths around 1.3 μm in quasi-CW Nd:YAG laser," *Opt. Laser Technol.* **94**, 112–118 (2017).
5. H. Y. Lin et al., "Nd:GYSGG laser at 1331.6 nm passively Q-switched by a Co:MgAl<sub>2</sub>O<sub>4</sub> crystal," *Opt. Mater.* **69**, 250–253 (2017).
6. X. F. Xu et al., "Relaxation oscillation suppressed, narrow linewidth, high beam quality, 1319 nm long-pulsed duration laser," *Appl. Opt.* **57**(16), 4692–4695 (2018).
7. A. Rolle et al., "Lobe-sparing resection of multiple pulmonary metastases with a new 1318 nm Nd:YAG laser—first 100 patients," *Ann. Thorac. Surg.* **74**(3), 865–869 (2002).
8. A. Rolle et al., "Is surgery for multiple lung metastases reasonable? A total of 328 consecutive patients with multiple-laser metastasectomies with a new 1318-nm Nd:YAG laser," *J. Thorac. Cardiovasc. Surg.* **131**(6), 1236–1242 (2006).
9. A. Rolle et al., "Laser resection technique and results of multiple lung metastasectomies using a new 1318 nm Nd:YAG laser system," *Lasers Surg. Med.* **38**(1), 26–32 (2006).
10. A. Kirschbaum, D. K. Bartsch, and P. Rexin, "Comparison of the local effects of a 600-μm bare fiber at high laser power on lung parenchyma: Nd:YAG laser 1320 vs. 1064 nm," *Lasers Med. Sci.* **32**(3), 557–562 (2017).
11. C. Porrello et al., "Pulmonary laser metastasectomy by 1318-nm neodymium-doped yttrium-aluminum garnet laser: a retrospective study

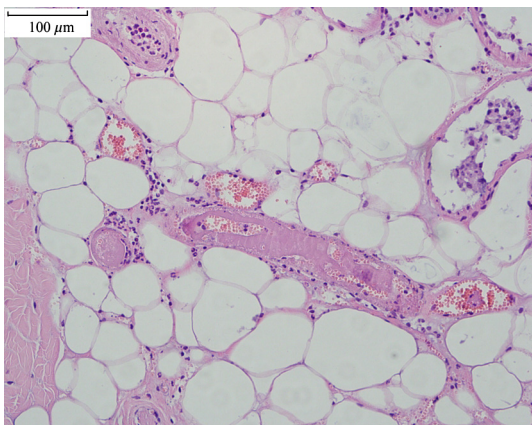


**Fig. 6** Histological sections of damaged skin fatty tissue at 48 h post exposure. Laser conditions: beam diameter 1.96 cm, exposure duration 3.0 s, and laser power 24.0 W.

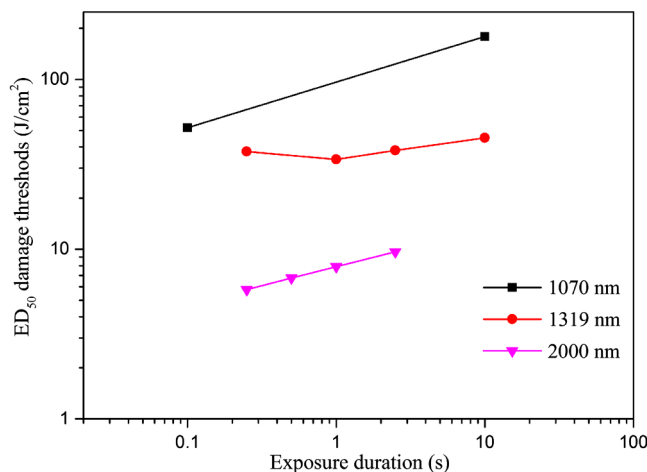


**Fig. 7** Comparisons of skin damage thresholds for 1070,<sup>37</sup> 1319,<sup>39</sup> and 2000 nm.<sup>32</sup> The 1/e<sup>2</sup> beam diameters for these wavelengths were all around 1.0 cm.

- about laser metastasectomy of the lung," *Surg. Innov.* **25**(2), 142–148 (2018).
12. M. Milanič and B. Majaron, "Energy deposition profile in human skin upon irradiation with a 1, 342 nm Nd:YAP laser," *Lasers Surg. Med.* **45**(1), 8–14 (2013).
  13. R. Liljemalm, T. Nyberg, and H. H. Von, "Heating during infrared neural stimulation," *Lasers Surg. Med.* **45**(7), 469–481 (2013).
  14. ANSI, *American National Standard for Safety Use of Lasers, Z136.1*, Laser Institute of America, Orlando, Florida (2014).
  15. D. H. Sliney et al., "What is the meaning of threshold in laser injury experiments? Implications for human exposure limits," *Health Phys.* **82**(3), 335–347 (2002).
  16. D. J. Lund et al., "Bioeffects of near-infrared lasers," *J. Laser Appl.* **10**(3), 140–143 (1998).
  17. L. G. Jiao et al., "Ocular damage effects from 1338-nm pulsed laser radiation in a rabbit eye model," *Biomed. Opt. Express* **8**(5), 2745–2755 (2017).
  18. B. Ketzenberger et al., "Study of corneal lesions induced by 1318 nm laser radiation pulses in Dutch belted rabbits (*Oryctolagus cuniculus*)," *Comp. Med.* **52**(6), 513–517 (2002).
  19. J. A. Zuclich et al., "Ophthalmoscopic and pathologic description of ocular damage induced by infrared laser radiation," *J. Laser Appl.* **10**(3), 114–120 (1998).
  20. J. R. Wang et al., "Corneal thermal damage threshold dependence on the exposure duration for near-infrared laser radiation at 1319 nm," *J. Biomed. Opt.* **21**(1), 015011 (2016).
  21. J. R. Wang et al., "Retinal thermal damage threshold dependence on exposure duration for the transitional near-infrared laser radiation at 1319 nm," *Biomed. Opt. Express* **7**(5), 2016–2021 (2016).
  22. H. X. Chen et al., "A comparative study on ocular damage induced by 1319 nm laser radiation," *Lasers Surg. Med.* **43**(4), 306–312 (2011).
  23. R. L. Vincelette et al., "Trends in retinal damage thresholds from 100 millisecond near-infrared laser radiation exposures: a study at 1110, 1130, 1150, and 1319 nm," *Lasers Surg. Med.* **41**(5), 382–390 (2009).
  24. R. L. Vincelette et al., "Thermal lensing in ocular media exposed to continuous-wave near-infrared radiation: the 1150–1350-nm region," *J. Biomed. Opt.* **13**(5), 054005 (2008).
  25. R. L. Vincelette et al., "Confocal imaging of thermal lensing induced by near-IR laser radiation in an artificial eye," *IEEE J. Sel. Top. Quantum Electron.* **16**(4), 740–747 (2010).
  26. E. L. Towle et al., "Quantification of thermal lensing using an artificial eye," *IEEE J. Sel. Top. Quantum Electron.* **20**(2), 158–165 (2014).
  27. R. Henderson and K. Schulmeister, *Laser Safety*, Taylor & Francis Group, New York (2004).
  28. M. H. Niemz, *Laser Tissue Interactions, Fundamentals and Applications*, Springer, New York (2004).
  29. X. Ma et al., "Bulk optical parameters of porcine skin dermis at eight wavelengths from 325 to 1557 nm," *Opt. Lett.* **30**(4), 412–414 (2005).
  30. H. Ding et al., "Determination of refractive indices of porcine skin tissues and intralipid at eight wavelengths between 325 and 1557 nm," *J. Opt. Soc. Am. A.* **22**(6), 1151–1157 (2005).
  31. E. Salomatina et al., "Optical properties of normal and cancerous human skin in the visible and near-infrared spectral range," *J. Biomed. Opt.* **11**(6), 064026 (2006).
  32. B. Chen et al., "Porcine skin ED<sub>50</sub> damage thresholds for 2,000 nm laser irradiation," *Lasers Surg. Med.* **37**(5), 373–381 (2005).
  33. B. Chen et al., "Modeling thermal damage in skin from 2000-nm laser irradiation," *J. Biomed. Opt.* **11**(6), 064028 (2006).
  34. B. Chen et al., "Histological and modeling study of skin thermal injury to 2.0 μm laser irradiation," *Lasers Surg. Med.* **40**(5), 358–370 (2008).
  35. J. W. Oliver et al., "Infrared skin damage thresholds from 1940-nm continuous-wave laser exposures," *J. Biomed. Opt.* **15**(6), 065008 (2010).
  36. C. P. Cain et al., "Visible lesion thresholds with pulse duration, spot size dependency, and model predictions for 1.54-μm, near-infrared laser pulses penetrating porcine skin," *J. Biomed. Opt.* **11**(2), 024001 (2006).
  37. R. Vincelette et al., "Porcine skin damage thresholds for 0.6 to 9.5 cm beam diameters from 1070-nm continuous-wave infrared laser radiation," *J. Biomed. Opt.* **19**(3), 035007 (2014).
  38. C. P. Cain et al., "Porcine skin visible lesion thresholds for near-infrared lasers including modeling at two pulse durations and spot sizes," *J. Biomed. Opt.* **11**(4), 041109 (2006).
  39. J. W. Oliver et al., "Infrared skin damage thresholds from 1319-nm continuous-wave laser exposures," *J. Biomed. Opt.* **18**(12), 125002 (2013).
  40. T. A. Eggleston et al., "Comparison of two porcine (*Sus scrofa domestica*) skin models for in vivo near-infrared laser exposure," *Comp. Med.* **50**(4), 391–397 (2000).
  41. L. G. Jiao et al., "Interaction of 1.319 μm laser with skin: an optical-thermal-damage model and experimental validation," *Proc. SPIE* **92301**, 923012 (2014).

**Luguang Jiao** received his BS degree in physics from Peking University in 2006. He received his MA degree and PhD in electro-optical engineering from the National University of Defense Technology in 2008 and 2013, respectively. His research interests are laser-tissue interactions and laser safety.

**Jiarui Wang** received her BS and MA degrees in photoelectric technology from the National University of Defense Technology in 2002 and 2006, respectively. She received her PhD in pathology from the Beijing Institute of Radiation Medicine in 2016. Her research interests are laser-induced ocular damage effects.

**Yan Fan** received her BS degree in bioengineering from Hubei University of Medicine in 2016. She received her MS degree in pathology from Anhui Medical University in 2019. Her research interests are laser-induced ocular damage effects.

**Zaifu Yang** received his BS degree in photoelectric technology from the National University of Defense Technology in 1996. He received his MS degree and PhD in pathology from the Beijing Institute of Radiation Medicine in 1999 and 2006, respectively. His research interests are laser-tissue interactions and laser safety.